Accurate ride comfort estimation combining accelerometer measurements, anthropometric data and neural networks

Cieslak, M. P., Kanarachos, S., Diels, C., Blundell, M., Baxendale, A. & Burnett, M.

Original citation & hyperlink:
Cieslak, MP, Kanarachos, S, Diels, C, Blundell, M, Baxendale, A & Burnett, M 2020, 'Accurate ride comfort estimation combining accelerometer measurements, anthropometric data and neural networks', Neural Computing and Applications, vol. 32, no. 12, pp. 8747–8762.

DOI 10.1007/s00521-019-04351-1
ISSN 0941-0643
ESSN 1433-3058
Publisher: Springer

The final publication is available at Springer via http://dx.doi.org/10.1007/s00521-019-04351-1

Accurate ride comfort estimation combining accelerometer measurements, anthropometric data and neural networks

M. Cieslak[12], S. Kanarachos[2], M. Blundell[2], C. Diels[2], M. Burnett[3], A. Baxendale[3]

Abstract

Ride comfort can heavily influence user experience and therefore comprises one of the most important vehicle design targets. Although ride comfort has been heavily researched there is still no definite solution to its accurate estimation. This can be attributed, to a large extent, to the subjective nature of the problem. Aim of this study was to explore the use of neural networks for the accurate estimation of ride comfort by combining anthropometric data and acceleration measurements. Different acceleration inputs, neural network architectures, training algorithms and objective functions were systematically investigated, and optimal parameters were derived. New insight in the influence of anthropometric data on ride comfort has been gained. The results indicate that the proposed method improves the accuracy of subjective ride comfort estimation compared to current standards. Neural networks were trained using data derived from a range of field trials involving ten participants, on public roads and controlled environment. A clustering and sensitivity analysis complement the study and identifies the most important factors influencing subjective ride comfort evaluation.

Key Words

Ride, Comfort Perception, Vibration, Neural Networks

1. Introduction

Ride comfort determines to a large extent a passenger's experience and therefore has been a heavily researched topic since the invention of the automobile[1]. In the last decade, the increasing number of embedded sensors and controllers on the vehicles has enabled car manufacturers to develop smart technologies that can adapt and personalise driving experience [2]. For example active suspensions can identify the road condition and automatically tune the suspension accordingly [3]. This opens an opportunity for personalising the suspension settings and adapting them to passenger preferences. Nowadays technologies such as adaptive suspension are used and prototypes of autonomous cars are being introduced and researched [4–6]. This requires redefining the analytical framework which is used for evaluation and tuning of ride comfort [7–9]. There have been various attempts to quantify the perception of ride comfort [10–18]. Majority of presented studies in the field of ride comfort have been conducted in laboratory environments [19–22] as in such conditions the inputs to the mechanical system can be easily controlled. Such an approach is highly desirable if the study requires investigation of specific parameters of the biodynamic characteristics of the human – seat system [23]. Another approach is to create a representation of the real-world conditions by simulating the environment, which allows achieving highly reproducible results and the possibility of investigating multiple driving scenarios with minimal expenditure[24–26]. Interpreting human reactions to vibration required creation of appropriate terminology and the introduction of different criteria for quantifying comfort or discomfort [27, 28]. The most common methods rely on objective measurements of vibration at the vehicle seat [29]. These measurements are usually done using accelerometers [30]. Whole body vibration research has led to the formulation of vibration tolerance criteria [14]. These criteria are the basis of the international standard that describes ride comfort - ISO2631[31]. The first iteration of the standard was published a couple of decades ago, and has been revised multiple times [14, 15]. The automotive industry has not agreed upon one uniform methodology for ride comfort testing [32–34]. Car manufacturers use different methods for their appraisal and development processes[35, 36]. A complete appraisal methodology consists of objective and subjective evaluation of a vehicle both on the proving ground and on public roads. A

[1] Corresponding author, email: cieslakm@uni.coventry.ac.uk, phone: +44 (0) 24 7635 5762
[2] Research Institute Future Transport and Cities, Coventry University, Priory Street, CV1 5FB, Coventry, UK
[3] HORIBA MIRA Ltd., Watling Street, CV10 0TU, Nuneaton, UK

variety of attributes are assessed [37], amongst which ride comfort can be described as the one with the highest complexity [38]. Ride comfort and its perception requires correlation of different types of data and ultimately it is subjectively assessed using a panel of vehicle engineers including noise vibration and harshness (NVH) specialists [39]. Due to the high level of variance of ride comfort perception among different people, it is hard to map subjective evaluations to ride comfort according to ISO 2631:1997 [40–42]. ISO 2631 only provides guidelines for determining the ride comfort. It has been agreed that the vibration frequencies most affecting ride comfort are those within the thresholds of 0.8 to 20Hz [43]. Researchers refer to the frequency thresholds from 0.8Hz to 5Hz as primary ride, and to those from 5Hz to 20Hz as secondary ride [44]. The frequency thresholds are freely interpreted by different manufacturers, so the definition is not consistent [45]. Vertical oscillations of a seated person at frequencies between 2Hz and 5Hz cause amplification of vibration within the body and therefore are perceived as more severe than vibrations at lower frequencies [46]. Studies have directly correlated the severity of mechanical inputs with the established perception thresholds [47]. Correlation of subjective and objective measures is usually conducted by statistical methods and thresholds described in ISO2631:1997 [48]. The correlation achieved is not of sufficient accuracy. On the other hand, Artificial Neural Networks (ANNs) are powerful mapping tools that can overcome such shortcomings. They have been used successfully in comfort prediction and for mapping subjective evaluations with objective measures [49, 50]. In this study we systematically explored the use of ANNs for the accurate estimation of ride comfort by combining anthropometric data and acceleration measurements. Different acceleration inputs, neural network architectures, training algorithms and objective functions were systematically investigated, and optimal parameters were derived. New insight in the influence of anthropometric data on ride comfort has been gained. The results indicate that the proposed method improves ride comfort evaluation compared to current standards. ANNs were trained using data derived from a range of field trials involving ten participants, on public roads and controlled environment. A clustering and sensitivity analyses complement the study and show how to detect outliers and identify the most important factors influencing ride comfort. The rest of the paper is structured as follows. Section 2 describes the guidelines contained within current standards for ride comfort estimation. Description of objective and subjective methods has been conferred. Section 3 presents experimental part of the study. In Section 4 the subjective and objective evaluation of ride comfort is analysed. Section 5 focuses on the neural network setup and methodology of testing. Conclusions have been presented in section 6.

2. Methods

Ride comfort is evaluated using subjective and objective measures [43, 51]. Complete methodology of ride comfort evaluation is described below.

2.1. Objective ride comfort measures

Objective ride comfort evaluation is currently performed using acceleration data and procedures described in the ISO 2631:1997, this is the standard for measuring whole body vibration in the ride comfort studies. The data set for each of the subjects and each of the measured road sections consists of an average weighted acceleration value, maximum transient vibration value (MTVV) and vibration dose value (VDV). According to the ISO standard and other research [52] these values can be used as predictors for ride comfort estimation. Since the perception of vibration is a nonlinear phenomenon and is much more sensitive to some frequencies a weighting filter must be applied. Such filters either reduce or enhance the spectral content of the measured vibration signal to replicate the typical human response to vibration exposure based on an empirical correlation [53]. Other comfort predictors are derived from the weighted acceleration values. Weighting curves from the ISO 2631 are presented in fig. 1. In the figure three curves are visible. W_k is used for weighting z-axis at the seat surface for health, comfort and vibration perception. W_d weighting curve is used for x and y-axis seat surface health, comfort and vibration perception weighting. Finally, the W_f is used primarily for motion sickness studies, which was not a scope of this experiment.

Before further processing the obtained signal is filtered using a 6th order Butterworth band-pass filter with cut-off frequencies at the lower limit set to 0.8Hz and at the upper limit to 200Hz. A running root mean square

(R.M.S.) method is used to calculate a_w, the weighted acceleration values (1). This method considers the occasional shock and transient vibration through the use of a short integration time constant.

$$a_w(t_0) = \left\{\frac{1}{\tau}\int_{t_0-\tau}^{t_0}[a_w(t)]^2 dt\right\}^2 \quad (1)$$

Where a_w represents weighted acceleration, τ represents the duration of the measurement.

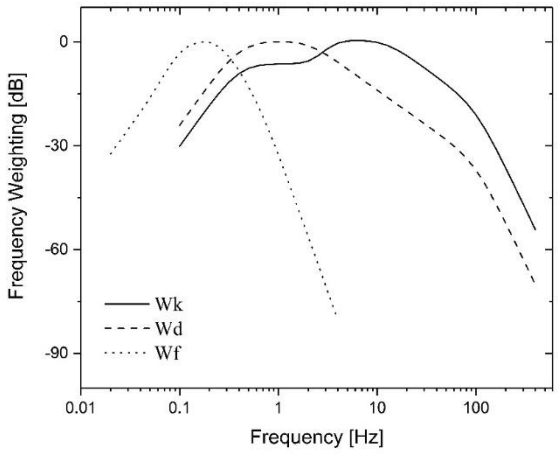

Fig. 1 Frequency weighting curves according to ISO 2631:1997

The maximum transient vibration value (MTVV) is calculated using (2). This value corresponds to the highest recorded magnitude of weighted vibration (a_w) during the measurement period.

$$MTVV = \max\left[a_w(t_0)\right] \quad (2)$$

Where $a_w(t_0)$ represents frequency weighted acceleration at time t_0.

The fourth power vibration dose method is more sensitive to peaks than a basic running R.M.S. averaging method (3). This evaluation method instead of using second power of the acceleration time history uses a fourth power for the basis of averaging. The vibration dose value (VDV) is expressed in metres per second to the power of 1.75 ($m/s^{1.75}$).

$$VDV = \left\{\int_0^T [a_w(t)]^4 dt\right\}^{\frac{1}{4}} \quad (3)$$

Where T represents measurement period and a_w is the frequency weighted acceleration at the time t.

2.2. Subjective ride comfort measures

Subjective measures of ride comfort were collected using questionnaires. The international standard for whole body vibration, ISO 2631, does not give any guidelines regarding the scale that should be used for subjective appraisal of ride comfort. Over the years a couple of different subjective scales were developed. Standard practice is to follow SAE J1060 [54] (fig. 2), which is also the case in this study.

1	2	3	4	5	6	7	8	9	10
UNACCEPTABLE				BORDER LINE	ACCEPTABLE				
CONDITION NOTED BY									
ALL OBSERVERS		MOST OBSERVERS		SOME OBSERVERS	CRITICAL OBSERVERS		TRAINED OBSERVERS		NOBODY
Intolerable	Severe	Very Poor	Poor	Marginal	Barely Acceptable	Fair	Good	Very Good	Optimal
1	**2**	**3**	**4**	**5**	**6**	**7**	**8**	**9**	**10**

Fig. 2 SAE J1060 subjective rating scale

In subjective ride comfort testing semantics plays a significant role. Due to the differences in perception between different people it is crucial to describe the movement of the vehicle in a way which is commonly recognised by all test subjects. There are terms which are frequently used amongst vehicle dynamics specialists. Low frequency motion of the vehicle with high amplitude of undulation is called primary ride and frequency threshold for this movement is recognised between 1-6Hz. Higher frequency, 6-15Hz, is described as secondary ride. Sudden movements due to existing potholes in the road surface cause sudden movement of the vehicle suspension and is by technical specialists referred to as jerk. These could not be used for this study, since some of the participants had very little experience in vehicle appraisal process. Therefore, a set of questions was constructed to simplify technical terminology. The test subjects participating in the study were asked to rate using the J1060 scale: 1) overall level of comfort, 2) the amount of high amplitude vertical vehicle motion, 3) the amount of small amplitude vibrations and 4) the amount of sudden vertical vehicle motions similar to the motion generated when hitting a pothole or a bump in the road surface. Prior to the subjective evaluation each subject was given detailed instructions on what to look for in each of the questions, as well as the overall description of each of the test sections used in the study.

3. Experiments and data collection

Field trials were conducted in a controlled environment at HORIBA MIRA proving ground in Nuneaton, UK, as well as on public highways using a chosen vehicle platform, described in the next subchapter. A detailed description of the experiments performed, and parameters recorded during the field trials are described in detail below.

3.1. Vehicle platform

The vehicle platform chosen for the experimentation consisted of a segment B vehicle – Ford Fiesta, model year 2013. This vehicle was chosen as a representative vehicle for the UK market. Although many studies conducted in the past have taken the parameters of the suspension of the vehicle platform into consideration – this was not the primary objective of this experiment, which was to collect subjective and objective ride comfort test for a variety of subjects, without changing the suspension characteristics. For purposes of the study, the vehicle was treated as a constant. To ensure the cohesiveness of the measurement, the number of variables was reduced

to a minimum. Influence of the tire sidewall deflection was also considered but was not identified as an influencing factor. To ensure high fidelity the tire pressure was set to manufacturer recommended value of 2.2 bar.

3.2. Field trials

Many ride comfort studies reported by researchers are conducted in a controlled environment, using vertical shakers, simulators and when possible digital representation of the dynamics systems is constructed, and the parametric studies are constructed to simulate the environment and the vehicle behaviour. Such studies offer great repeatability and reproducibility of the results as well as great level of controllability of the input parameters. Although field studies in ride comfort do not provide such level of confidence in the results, they are key to fully investigate the human-vehicle interaction due to inability to fully simulate real-world conditions in a laboratory or simulated environments. In this paper authors present experimental methodology used for ride comfort evaluation. For such experimentation five different routes were chosen (table 1). Three road sections were located within the proving ground and two were sections of a public road.

Table 1 Road sections used for data collection

Name	**Type of road**	**Type of inputs**
Battlefield road	Public	Primary and secondary ride inputs. Range 1-10Hz.
Fenn lanes	Public	Primary ride inputs. Range 1-5Hz.
Circuit no. 1	Proving ground	Secondary ride inputs. Range 8-12Hz.
Circuit no. 2	Proving ground	Secondary ride inputs. Range 5-12Hz.
Ride & handling circuit	Proving ground	Primary and secondary ride inputs. Range 1-10Hz.

The frequency content of each road section is illustrated in figure 3. The different road sections are characterised by a different frequency signature. Information about the vibration on each of the sections was collected using triaxial accelerometers installed on the vehicle wheel hubs and connected to a LMS SCADAS data acquisition system. To create PSD (Power Spectral Density) of the vibration signal and to compare them, the signals were filtered using a Butterworth bandpass filter with a filtering threshold between 0.8-150Hz. Additionally, the PSD was converted to a one third octave band format. This can be observed on the PSD graph, shown in fig. 3.

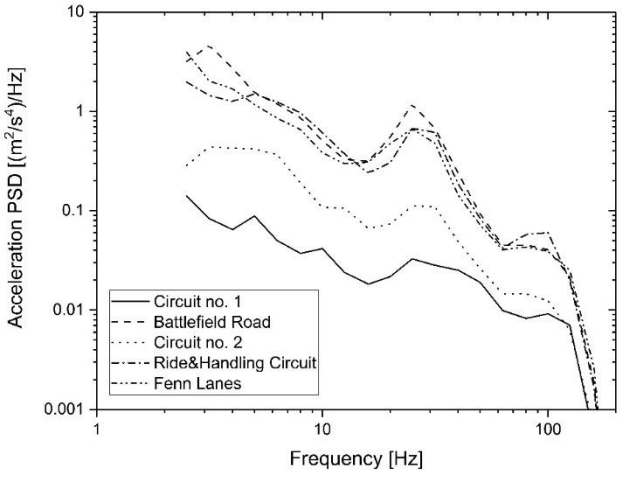

Fig. 3 Power spectral density of signals acquired over different road sections

Based on the information within the figure the smoothest road section chosen for the experiment was the Circuit no. 1, followed by Circuit no. 2. The measured vibration magnitude on the Ride and Handling circuit, the

Battlefield Road and the Fenn Lanes sections were much more severe. It can be observed that low frequency high amplitude vibration was generated on both Ride and Handling circuits, which were used for primary ride component estimation, and Battlefield Road section has high magnitude vibration level between 10-18Hz, therefore can be used for secondary ride component evaluation. According to the ISO standard, which is based on acceleration data, different ride comfort perception should be experienced for each road category. However, according to the ISO standard, there shouldn't be any differences among the subjects' perception.

The variables measured during the field trials were acceleration measurements at 7 different locations on the vehicle. The equipment used for data logging and the location of each accelerometer is presented in table 2.

Table 2 Location of accelerometers on the test vehicle

No.	Equipment	Location
1	Triaxial DeltaTron 4525	Left front wheel hub
2	Triaxial DeltaTron 4525	Right front wheel hub
3	Triaxial DeltaTron 4525	Left rear wheel hub
4	Triaxial DeltaTron 4525	Right rear wheel hub
5	Triaxial DeltaTron 4525	Passenger seat rail
6	Triaxial DeltaTron 4515-B	Passenger seat pad
7	Triaxial DeltaTron 4515-B	Passenger seat back

The LMS SCADAS Data Acquisition system was used for data logging. The data logger was connected to a laptop using an Ethernet connection. The vibration in the vehicle was measured using three accelerometers mounted in the vehicle: on the seat pad, at the seat back and on the seat rail. Accelerations were measured in the X, Y, Z direction at a 1024Hz sampling rate. One accelerometer was mounted on the inner side of each of the wheel hubs - total of 4.

The participants were asked to adjust the seat to a position in a way that in their opinion provided them with the highest level of support and the highest possible level of comfort at that moment. Each of the subjects was introduced to the testing procedure. The procedure involved one familiarisation run on each of the road sections. After familiarisation two data collection runs were performed. During the subjective evaluation runs objective measures – accelerations, were recorded for all the subjects.

3.3. Anthropometric data collection

For the purposes of this study 10 participants were chosen from HORIBA MIRA staff. Before conducting the field trials, appropriate ethics approval (project ref. P71148) from Coventry University ethics board was received. Number of participants varies between different studies ranging from 5-10 participants [55], through 20-30 [56, 57]participants to extreme numbers of 3000 test participants in experiments conducted by NASA[58]. The number of participants was chosen based on the fact that the planned tests were to be conducted not in laboratory environment but on the proving ground, and due to budget limitations the final number of participants has been limited to 10 (N=10). The participants were asked to fill in a questionnaire, requiring anthropometric data such as their height, weight and age. The participants were also asked to mention if they had motion sickness record, since there was a possibility of subjects feeling ill during the course of the study. These parameters are listed in table 3, under the HMS column and were evaluated on the scale from 0 to 10. Another field of interest was any previous experience in vehicle dynamics subjective appraisal methodology. This data is shown (table 3) as the EXPinVD parameter. The body mass index (BMI) parameter was calculated using equation 4.

$$BMI = \left\{\frac{mass_{kg}}{height_{cm}^2}\right\} \tag{4}$$

Based on the collected data, a final pool of human subjects was chosen. The data for those ten participants is presented in table 3.

Table 3 Anthropometric and experience data of selected test participants

Subject	Gender	Age	Height (cm)	Weight (kg)	BMI	EXPinVD	HMS
1	Male	25	178	60	18.9	3	5
2	Male	23	180	72	22.2	7	1
3	Male	61	193	107	28.7	8	2
4	Male	40	176	90	29.1	3	3
5	Female	32	158	55	22	1	1
6	Male	30	191	86	23.6	7	1
7	Male	68	183	83	24.8	10	1
8	Male	43	172	70	23.7	4	4
9	Male	31	176	74	23.9	7	7
10	Male	25	182	79	23.8	4	1

During the study additional anthropometric parameters were collected to characterise the overall sizes of each subject within the test group the population for statistical analysis. Therefore, the following parameters were collected (table 4).

Table 4 Anthropometric measures collected

Parameter	Abbreviation	S1	S2	S3	S4	S5	S6	S7	S8	S9	S10
Standing height	SH	176	178	193	176	158	191	183	172	176	181
Sitting height	SiH	100	108	113	109	98	112	110	102	103	105
Sitting shoulder height	SiSH	76	79	83	76	56	82	79	82	73	77
Buttock popliteal length	BPL	38	52	59	53	48	57	54	49	57	56
Knee height	KH	55	58	58	56	40	57	50	47	50	47
Shoulder breadth	SB	40	47	52	48	38	44	49	42	45	48
Hip breadth	HB	31	36	48	47	32	34	39	40	36	42

As per table 3, N=10 subjects participated in the study. The parameters considered were: Age (Min=23, Max=68, Mean **37.8**, SD=**15.53**), Height (Min=158, Max=193, Mean=**178.9**, SD=**9.86**), Weight (Min=55, Max=107, Mean **77.6**, SD=**15.06**), BMI (Min=18.94, Max=29.05, Mean **23.76**, SD=**3**), EXPinVD (Min=1, Max=10, Mean **5.5**, SD=**2.80**) and HMS (Min=1, Max=7, Mean **1.5**, SD=**2.12**). Although gender parameter was recorded and reported in this study, it has not been taken into consideration in further data processing. For subjective score reporting male participants tend to score fewer extreme values, which results in lower variability of reported values. Gender may play a role when considering physical differences, as with females generally there is more fat tissue in the upper torso, which in vibration studies results in different transfer functions[59, 60]. This has been tested and is reported in section 4 of this paper, figure 10. No significant difference between female subject and the male subjects was found. Additionally, anthropometric parameters of body size were recorded for all test participants. The parameters included: standing height (mean=178.4, SD=9.35), sitting height (mean=106, SD=4.90), sitting shoulder height (mean=76.3, SD=7.40), buttock popliteal length (mean=52.3, SD=5.83), knee height (mean=51.8, SD=5.69), shoulder breadth (mean=45.3, SD=4.12), and hip breadth (mean=38.5, SD=5.55).

4. Ride comfort analysis

Subjective and objective comfort measures were analysed with respect to ISO 2631-1:1997 standard. The objective measures of weighted acceleration magnitude for each subject on each road section is illustrated in fig.

4. Calculated weighted acceleration for each of the road sections is shown in the figure 4. The perception thresholds which are included in the ISO2631:1997 are shown in table 5.

Table 5 Likely reaction to vibration magnitude according to ISO 2631:1997

Weighted acceleration magnitude a_w [m/s^2]	Likely reaction when exposed to vibration
<0.315	not uncomfortable
0.315 – 0.630	a little uncomfortable
0.50 – 1.00	fairly uncomfortable
0.80 – 1.60	uncomfortable
1.25 – 2.50	very uncomfortable
>2.00	extremely uncomfortable

In the gathered data set none of the sections exceeded a weighted magnitude acceleration of 1.1 m/s^2. Based on the objective results it can be assumed that when compared the most comfortable section of road was located on the Circuit no. 1 of the HORIBA MIRA proving ground. When collated with the likely reactions to vibrations of certain magnitude used road sections can be put in order from the most comfortable one to the least comfortable one, which is shown on table 6.

Table 6

Comfort rating number	Road Section
1 – highest perceived comfort	Circuit no. 1
2	Circuit no. 2
3	Ride & Handling Circuit
4	Fenn Lanes
5 – lowest perceived comfort	Battlefield Road

There is very little difference in the measured weighted acceleration magnitudes on the public sections of road. Both of these roads are characterised by high magnitudes of vibration at 0.8 m/s^2, which is described in the standard as either fairly uncomfortable or uncomfortable. For further investigation of the vibration dose value (VDV) results was undertaken for both the seat pad and the seat rail locations. The results are presented in the figure 5.

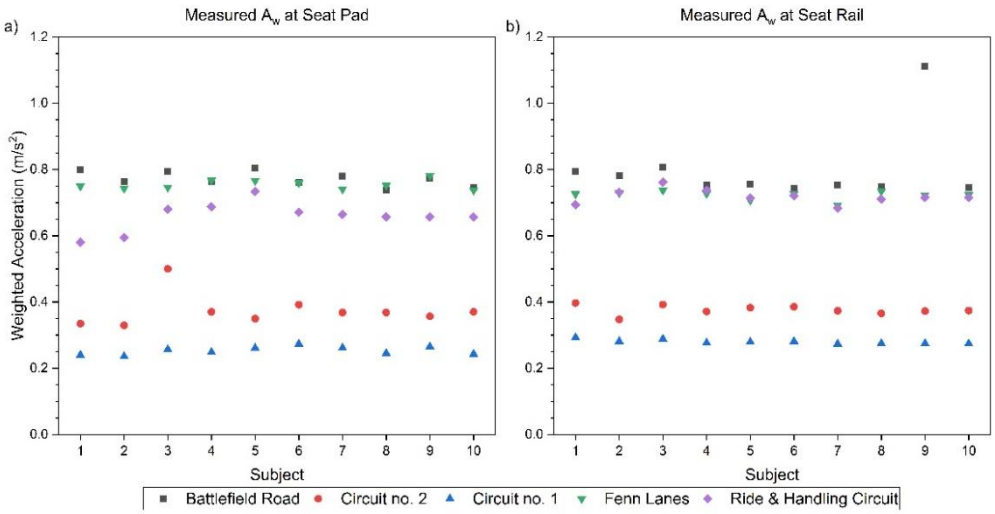

Fig. 4 Weighted acceleration magnitude for each participant on each road section a) measured at the seat pad b) measured A_w at the seat rail

By comparing the calculated results of the VDV for each of the participants on different road sections it is visible that the highest VDV was achieved when driving on the Fenn Lanes section of the public road. When compared with the results obtained by calculating the weighted acceleration magnitude it can be seen that the highest level of discomfort should be perceived on the Fenn Lanes section of the public road, followed by the Battlefield Road and the Ride and Handling Circuit.

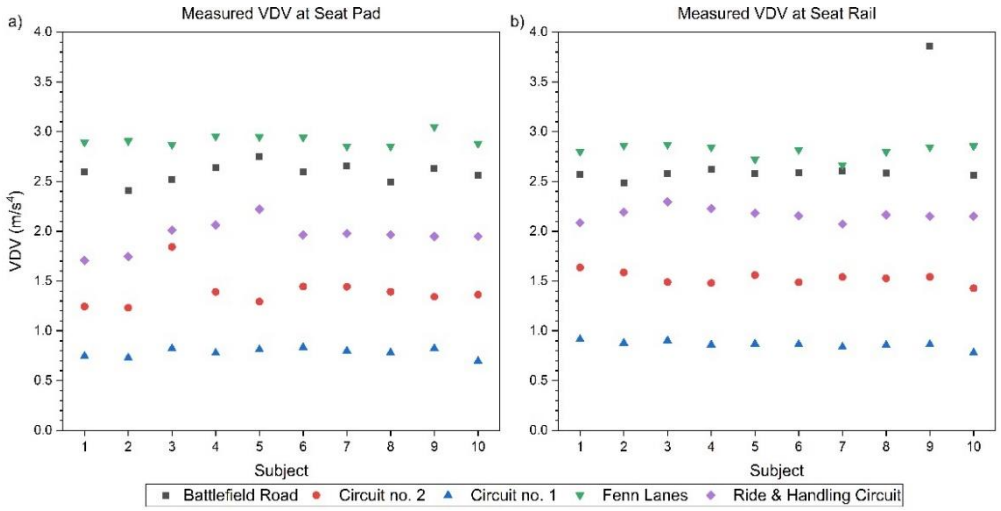

Fig. 5 Measured VDV for different test participants at seat pad and seat rail on different road sections. a) VDV at seat pad, b) VDV at seat rail

When compared with the Power Spectral Density (fig. 3) calculated for each of the road sections it is visible that Fenn Lanes section of the public road has the higher power of the frequency component of the vibration signal between 2-4Hz, so in general it will produce more low frequency, high amplitude vibration. The Battlefield Road has higher power spectrum of vibration between 6-15Hz, which is referred to in technical terms, as secondary ride. Therefore, the final classification of road sections with respect to the perceived comfort, according to ISO2631:1997 guidelines, is shown in the table 7.

Table 7 Section of road used for testing in order of measured comfort value corrected by using VDV calculations

Comfort rating number	Road Section
1 – highest perceived comfort	Circuit no. 1
2	Circuit no. 2
3	Ride & Handling Circuit
4	Battlefield Road
5 – lowest perceived comfort	Fenn Lanes

These findings were compared to the subjective results obtained through the questionnaire. The results of the subjective ride comfort evaluation can be seen in fig 6 to fig. 9. The results are divided into 4 different graphs (fig. 6 to 9) representing each question asked within the subjective questionnaire.

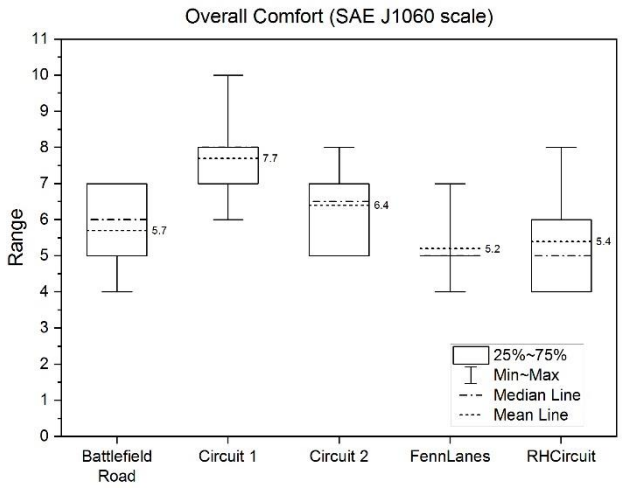

Fig. 6 Subjective comfort responses. Overall perceived comfort on the test road sections.

In fig. 6 the response to questions about the general comfort condition for each of the measured sections of the road is shown. The highest comfort, subjectively, was recorded on Circuit no. 1 (mean 7.7), and followed by Circuit no. 2 (mean 6.6), Battlefield Road (mean 5.7), Ride and Handling circuit (mean 5.4). The lowest scoring road section among trial participants was the Fenn Lanes section of the public road. The general comfort results, although showing some correlation with the objective data, do not provide any insight into the specific ride comfort components perceived on these road sections. Two parameters which are important in vehicle ride characterisation are primary ride and secondary ride.

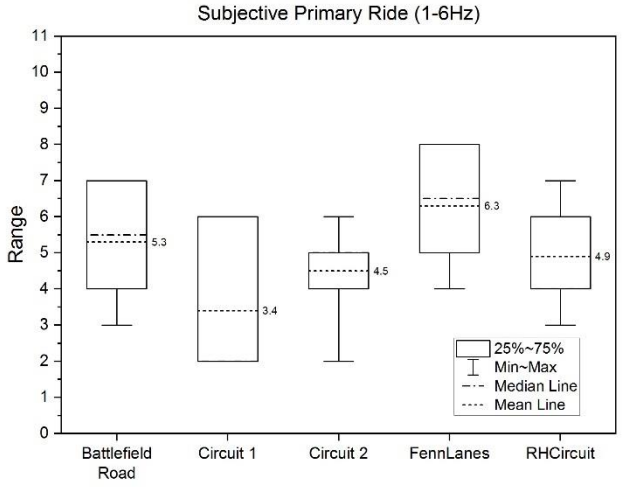

Fig. 7 Results of the subjective perceived amount of primary ride vibration 1-6Hz.

These two attributes were described as the amount of vertical vehicle motion (primary ride), sudden vertical vehicle motion and the severity of small amplitude vehicle vibration for secondary ride and jerk/chop motion. These three parameters have been characterised by the trial participants and the results are shown on the fig 7, 8 and 9. Circuit no. 1 section of the proving ground, according to the subjective evaluation, has the lowest score for primary ride motion (mean result 3.4). This motion can be described as low frequency, high amplitude motion. Such result was expected due to the surface of this proving ground section which is comparable to a motorway grade surface. The highest score was for the subjective evaluation of primary ride was recorded on the Fenn Lanes section (mean score of 6.3).

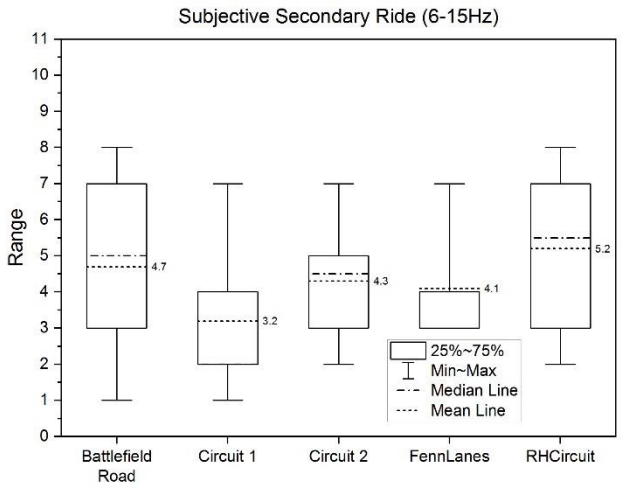

Fig. 8 Results of the subjective perceived amount of secondary ride vibration 6-15HzHz.

The secondary ride results show very high variance in the responses of the subjects. The highest secondary ride mean results were recorded on Battlefield Road and Fenn Lanes sections of the public road and on the Ride and Handling circuit of the HORIBA MIRA proving ground. Additionally, to standard ride comfort questions, test participants were asked about the amount of whole-body motion in the vehicle and the amount of head motion due to the amount of vibration being transmitted to their head.

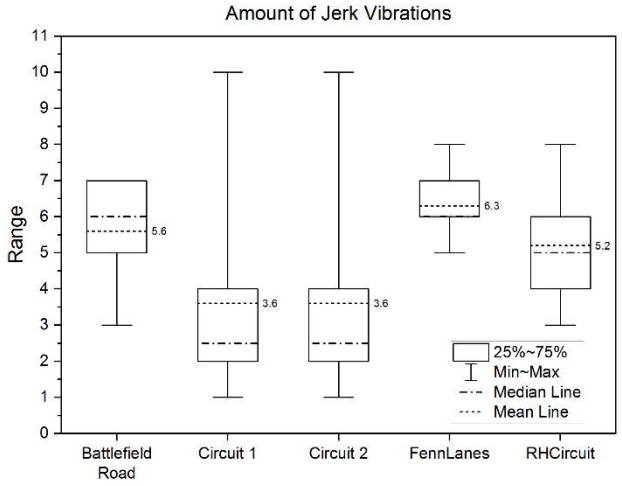

Fig. 9 Secondary ride, perceived jerk and impact vibration.

Mean values of these suggest that the vehicle has a stiff suspension setup tuned for good handling and good road holding. On all the graphs the minimum and the maximum values along with the two middle (25-75%) percentiles are shown. Variability of responses for the same road section among different test participants is visible. Using the mean values of the obtained data sets is not an ideal methodology due to high variance of the data and the differences between the subjects both in terms of their experience and bio mechanics of their bodies. To further investigate the inter-subject variability due to changing apparent mass when undergoing vibration excitations, the floor to thigh transmissibility (fig. 10) for each of the subjects on the Fenn Lanes road sections was calculated using the equation (5) [29, 46, 61],

$$H(f) = \frac{G_{io}(f)}{G_{ii}(f)} \tag{5}$$

Where the transmissibility is defined as the ration of the vibration on the seat surface to the vibration at the seat base (usually the floor of the vehicle – in the field trials the seat rail was used instead). In the equation 5 the $G_{io}(f)$ is the acceleration at the seat in the frequency domain and the $G_{ii}(f)$ is the acceleration at the vehicle floor.

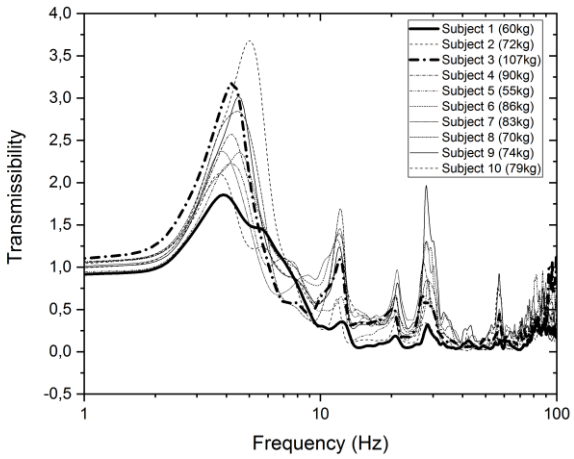

Fig. 10 Apparent mass transmissibility for subjects involved in the study on Fenn Lanes road section.

This road section was chosen due to highest inputs in low frequency region as per PSD graph shown in fig. 3. In graph 6 it is visible that first resonance mode for the vibration acting on passengers inside of the vehicle platform is occurring between 4-5Hz and is the highest influencing factor of perceived comfort. It is also visible that for subjects of varying mass the transmissibility is different. In bold results for Subject 1 and 3 are shown.

The discrepancy motivated more personalised approach to solving this correlation problem. Therefore, a machine learning approach was taken. The use of a neural network that can handle multiple inputs and multiple outputs can be used to greatly speed up the process of finding and analysing patterns in the data set.

5. Ride comfort estimation model

Collected and analysed ride comfort data was used to create ride comfort estimation model based on artificial neural networks. This model is described below.

5.1. Artificial Neural Networks and ride comfort

Some studies in the past have investigated the feasibility of Artificial Neural Networks for vehicle ride comfort estimation and prediction. One of the first studies, which investigated usability of Artificial Neural Networks for subjective response prediction was conducted by Kolich at University of Windsor in Canada. He looked at the possibility of using them as a correlation method for objective and subjective seating metrics [50], the developed model was then assessed and compared with a statistical study [62], which led to proposal of a formalised framework for standardised seat comfort tests [9]. In his work the main objective was to assess the seating comfort derived mainly from subjective responses and pressure mapping of the subjects interacting with the seat. Another example of use of Artificial Neural Networks for vehicle dynamics work includes control of active and adaptive suspension systems for improvement of vehicle ride comfort. Cases of such work have been presented by Eslaminasab [63] in her work on suspension fuzzy control approach using neural networks for heavy

vehicles. Other examples of using the artificial neural networks approach for ride comfort evaluation and prediction have been presented by Lerspalungsanti S. [64, 65]. He explored methodologies for subjective evaluation in electric vehicles using artificial neural networks as well as prediction model of ride comfort for drivetrain vibrations. Gao et al [66] in his study utilised ANNs to predict vehicle ride comfort based on the octave band vibration values recorded from a vehicle. In his methodology instead of recording the subjective responses he compared them directly with the chart from the ISO2631 standard, as presented in this paper in table 5, which does not provide any insight in what the actual subject responses of the people in the vehicle might be. Another example of using supervised learning for ride comfort estimation in a laboratory environment is a study conducted at Concave research centre in Canada by Taghavifar et al.[67], where the neural networks were used as a tool for apparent mass estimation and prediction tool. As ANNs can be used for discovering nonlinear correlations between parameters, Nybacka et al, used them to correlate objective metrics for steering with the obtained driver ratings [68]. The reviewed papers utilise neural networks for correlation of highly nonlinear parameters. Therefore, it has been decided that similar approach will be taken, and the developed model will utilise the advantages of using the neural networks. The development of a model used in this study is presented in the following subchapters.

5.2. Neural network model for ride comfort

Artificial Neural Networks have been developed as generalisations of mathematical models of biological nervous systems [69]. The basic elements of a neural network are artificial neurons which are also referred to as nodes. The connections between the neurons are represented by weights that modulate the input signals. The non-linear characteristic of a set of neurons is usually represented by a transfer function [70]. The neuron impulse is calculated as a weighted sum of the inputs to the neuron, transformed by its transfer function. The learning capabilities of the neural network are achieved by adjusting the weights in accordance to chosen learning algorithm. The working principle of a neural network can be expressed mathematically as (6):

$$a^{(1)} = \sigma\left(\begin{bmatrix} W_{0,0} & \cdots & W_{0,n} \\ W_{1,0} & \cdots & W_{1,n} \\ \vdots & \ddots & \vdots \\ W_{k,0} & \cdots & W_{k,n} \end{bmatrix}\begin{bmatrix} a_0^{(0)} \\ a_1^{(0)} \\ \vdots \\ a_n^{(0)} \end{bmatrix} + \begin{bmatrix} b_0^{(0)} \\ b_0^{(0)} \\ \vdots \\ b_n^{(0)} \end{bmatrix}\right) \tag{6}$$

This can be shortened and expressed as (7):

$$a^{(1)} = \sigma(Wa^{(0)} + b) \tag{7}$$

Where σ – is the logistic activation function, W represents the weights of the neural network and b the biases.

The firing of the neuron is dependent on the state of the activation function. There can be different activation functions used in a neural network. The simplest activation function is the logistic activation function $\sigma(x)$ (8) which has been used in this case study.

$$\sigma(x) = \frac{L}{1+e^{-k(x-x_0)}} \tag{8}$$

Where L represents the curves maximum value, k steepness of the curve, x_0 function's midpoint and e is the Euler's number.

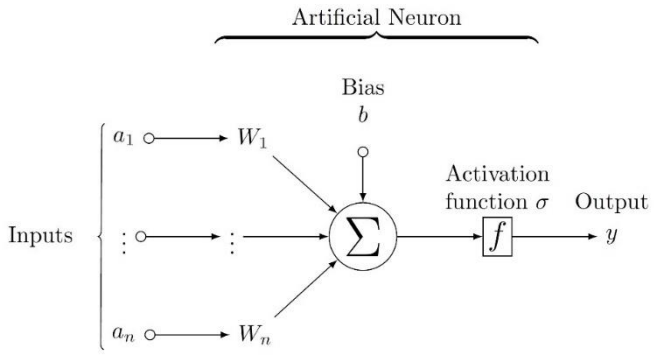

Fig. 11 Schematic of a single neuron in a neural network

Different training functions and algorithms were explored for this study. Back Propagation Artificial Neural Network was used utilising a Levenberg-Marquardt (LM) algorithm (9), (10) and a Scaled Conjugate Gradient (SCG) algorithm. The LM algorithm is a popular alternative to the Gauss-Newton method of finding the minimum of training function $F(x)$.

$$F(x) = \frac{1}{2}\sum_{i=1}^{m}[f_i(x)]^2 \tag{9}$$

where $F(x)$ is the mean squared error (MSE). Let the Jacobian of $f_i(x)$ be denoted as $J_i(x)$, then the LM method searches in the direction given by the solution p to the equation (9):

$$(J_k^T J_k + \lambda_k I)p_k = -J_k^T f_k \tag{10}$$

Where λ_k are nonnegative scalars and I is the identity matrix [71].

The scaled conjugate gradient (SCG) algorithm is too complex to describe in detail in this paper. The full description and working principles of that algorithm has been presented by Møller [72]. The first of the mentioned above computational techniques, the LM method is one of the fastest available and it is highly recommended as a first-choice for training Artificial Neural Networks. The downside of using this method is the fact that it finds only a local minimum which does not necessarily happen to be a global minimum. The LM method is more robust than the SCG algorithm, and it tends to find the solution even when it starts far off from the error minimum. A SCG algorithm on the other hand performs an adjustment of weight along conjugate direction. This is motivated by the desire to accelerate the typically slow convergence associated with gradient descent. Two different methods for calculating the error were used in the study. The first one was a mean squared error (MSE) algorithm which can be expressed as (11):

$$MSE(\widehat{\Theta}) = E\left((\widehat{\Theta} - \Theta)^2\right) \tag{11}$$

Where $\widehat{\Theta}$ is an estimator of the parameter Θ. The MSE can be written as sum of variance and the squared bias of the estimated (12):

$$MSE(\widehat{\Theta}) = D^2(\widehat{\Theta}) + \left(b(\widehat{\Theta})\right)^2 \tag{12}$$

Where D^2 the variance of the estimator is $\widehat{\Theta}$, $b(\widehat{\Theta})$ is the bias of the estimator.

The second method used for error calculation was the mean absolute error (MAE), which can be expressed as (13):

$$MAE = \frac{\sum_{i=1}^{n}|y_i - x_i|}{n} = \frac{\sum_{i=1}^{n}|e_i|}{n} \tag{13}$$

Where y_i and x_i are the coordinates of the data on XY scatter plot, e_i stands for absolute error.

The most common architecture of a neural network consists of an input, a hidden layer (or multiple hidden layers) and outputs. Besides the architecture of the neural network, the process followed to update the neural network weighting factors is equally important. Learning in neural networks can be classified into three different

types: supervised learning, unsupervised learning and reinforced learning Abram et al. [73]. In the work described here the neural networks were trained using the first method. Supervised learning is an iterative process in which known inputs and outputs are provided by the external teacher. In the first iteration random weights are assigned to the neural network and an error between the neural network and the real output is formed. To find out which way the error created by the network is progressing it is necessary to calculate the partial derivative of the weights of the network. A positive or negative sign of the derivative of the weight tells us whether the error of the node is approaching its local minimum or is approaching the maximum. In the backpropagation algorithm calculation and an addition of the calculated derivatives to the weights progresses from the output layer, through the hidden layer to the input layer – in the backward movement. It has been proven that a backpropagation neural network with enough hidden layers is capable of approximation of any non-linear function.

5.3. Ride comfort training data

For the purposes of this study an evaluation of different road sections with different people was made. The data was prepared to be used in the neural network training process. The inputs in equation (14), (15) and outputs in equation (16) have been prepared to be used in the neural network training process. A greater number of inputs, than the described minimum in the ISO2631:1997, was used in the input matrix. This data also included the anthropometric measurements of the test participants.

$$I_i = [SH \quad SiH \quad SiSH \quad BPL \quad KH \quad SB \quad HB \quad Weight \quad BMI \quad A_{wx} \quad A_{wy} \quad A_{wz} \quad MTVV_x \quad MTVV_y \quad MTVV_z \quad VDV_x \quad VDV_y \quad VDV_z]^T \tag{14}$$

$$inputs = [I_1 I_2 I_3 I_4 \cdots I_{50}] \tag{15}$$

$$outputs = [SCV_1 SCV_2 SCV_3 SCV_4 \cdots SCV_{10}] \tag{16}$$

The output (15) consisted of the subjective evaluation results (SCV = Subjective Comfort Value) of test participants collected on each of the road sections. The dataset used in the neural network training consisted of data recorded from 10 subjects, where 3 repetitions of each data recording were taken. The data was logged on 5 sections of road. The number of individual samples used for training equalled 150, where each sample contained 19 parameters describing the ride comfort. Overall number of parameters in the dataset equalled 2850.

5.4. Artificial Neural Network training for ride comfort

The neural network was then trained using the data set. Neural network training was performed using MATLAB. As aforementioned, two different training algorithms were tested: LM (9) and SCG. Two methodologies for calculating the error function were tested the Mean Squared Error (MSE) (12) and Mean Absolute Error (MAE) (13). To optimize the hidden layer size, the size varied between 15 and 40 neurons with a step size of 1. This approach was implemented for each of the networks. Then systematically each network was trained 30 times. For each of the created networks R correlation value was recorded. It is well known that Artificial Neural Networks can converge into local minimum and not in the desired global minimum. To limit this behaviour two algorithms were implemented. Small perturbation in the weights was introduced and the network was then restarted and retrained. Such methodology is often referred to as noise injection. It is a known methodology to avoid overtraining of the artificial neural network, especially when the dataset is relatively small, as it is in this case. The noise injection has been implemented between the training cycles. Such approach allows the correlation function to escape from local minima. In the study two different types of perturbation were tested. The results are from each perturbation are labelled M1 and M2, results labelled M0 are from a neural network that did not have this feature implemented (fig. 12 to 14).

5.5. Results and sensitivity analysis

The results shown from fig. 12 to fig. 14 show the best regression results from the different neural networks tested during the study. The best result was obtained using the LM algorithm and MSE method as the training function. The R value achieved for that network was 0.95, which means that there is a high correlation between results predicted by this particular network and the subjective ride comfort evaluations Fig. 12 shows the best regression outcomes without perturbation (M0) and for two different levels of perturbation (M1 and M2). The overall performance of those networks fluctuates around 0.9 regardless of the size of the hidden layer used.

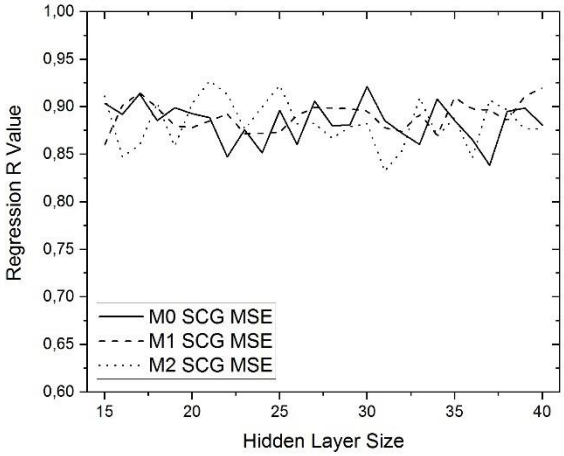

Fig. 12 Regression results for varying hidden layer size, SCG algorithm with MSE performance function

Fig. 13 refers to network with the same backpropagation algorithm (SCG) but different performance function (MAE). The graph shows that overall performance of the resultant network is worse than the one presented in fig. 8a. The perturbation algorithm improved the results for a higher number of neurons (33-40).

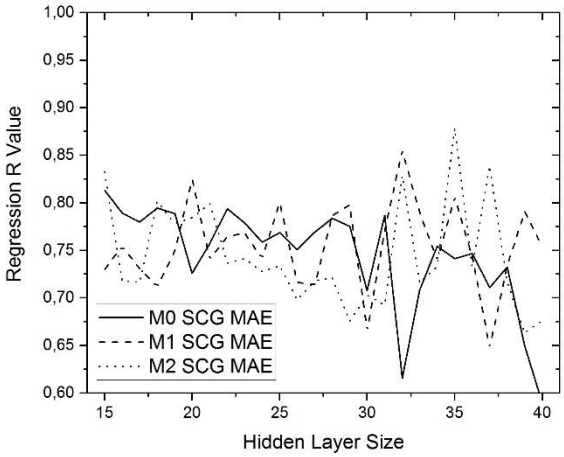

Fig. 13 Regression results for varying hidden layer size, SCG algorithm with MAE performance function

Fig. 14 refers to network based on LM backpropagation algorithm. This type of network showed the best overall performance. Implementation of perturbation in the weights improved the networks performance with hidden layer size ranging from 24 to 30 and from 35 to 40.

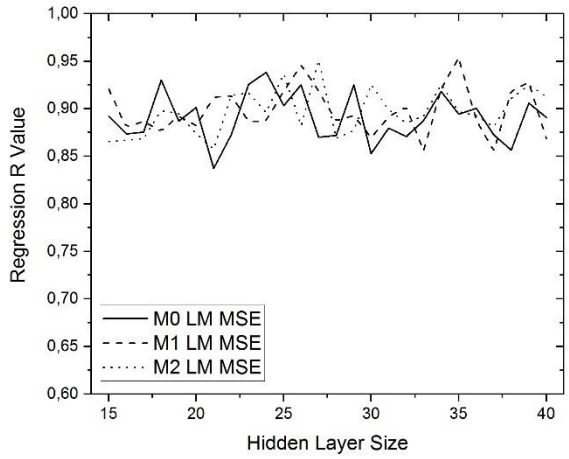

Fig. 14 Regression results for varying hidden layer size, LM algorithm with MSE performance function

In all cases, as observed, the perturbation algorithm achieved similar results with those achieved without perturbation but with a fewer number of neurons.

For the best performing network, a sensitivity analysis was performed (fig. 15). The analysis shows that the resulting network is most sensitive to changes in the values of sitting height and the vertical axis weighted acceleration. The network is least sensitive to changes in values of weight, vibration, maximum transient vibration and vibration dose values in the X and Y direction. These conclusions fit in with current methodologies where emphasis is put on measurements in Z axis direction. Results measured in the Z axis direction are considered as highest influencing factor in ride comfort perception.

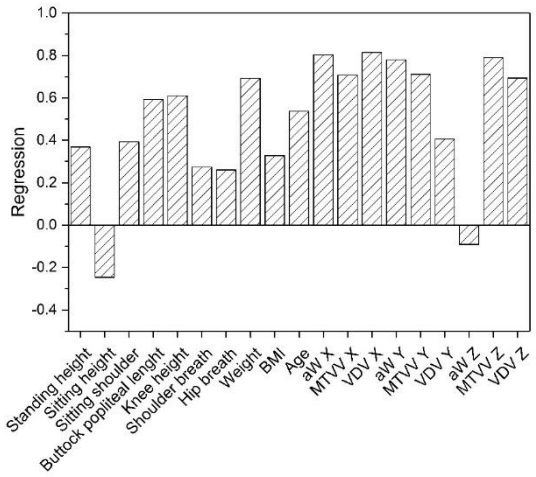

Fig. 15 Results of sensitivity analysis

Fig. 16 presents the error between the input and output data. The subjective evaluation was scored using the SAE J1060 standard [54], which is utilising 10 point comfort scale (fig. 2). This means that neural networks predicted value in some cases was off by 15-20%. Considering the fact that only 10-point scale is used, this is a considerable error. In the future it would be more recommended to use different subjective response measurement scale for example a variant of Borg100 which is a non-linear 100-point discomfort scale. Nevertheless, results obtained with SAEJ1060 are within acceptable limits for vibration evaluation in vehicles.

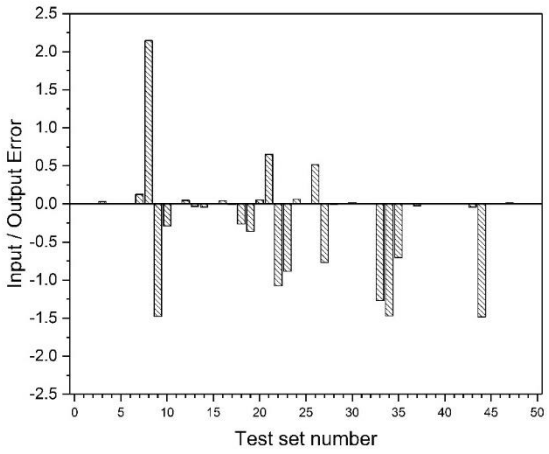

Fig. 16 Error between predicted output values and actual measured output values

6. Conclusions and future work

In this study, a ride comfort evaluation and estimation methodology are presented. Nowadays, the shift towards personalisation requires the re-evaluation of current work flows and methods used in the automotive industry. Field trials were conducted on five different road sections. Ride comfort was evaluated using acceleration measurements, ISO 2631, and subjective evaluations according to SAE J1060. Ten subjects (N=10) have participated in the study. Although the objective metrics were aligned, significant differences emerged in the subjective assessment. For the accurate prediction of subjective ride comfort evaluation, a neural network approach was employed. In this study feed-forwards networks were trained. To fully investigate the impact of different neural network parameters, performance functions and cost function a parametric study was desiged. Optimisation of the hidden layer size was performed. The hidden layer size ranged from 15 to 40 neurons. Two gradient descent-based algorithms (Levenberg-Marquardt and Scaled Conjugate Gradient) and two error calculation techniques (mean absolute error and mean squared error) were tested. Additionally, algorithms preventing overtraining, such as noise injection were introduced during training. Through used methodology an optimal neural network for objective and subjective parameter correlation was derived. The best performing artificial neural network comprised of 34 neurons in the hidden layer. In this network noise was injected to the weights of the network, to avoid overtraining due to small sample size. Training was accomplished using Levenberg-Marquardt backpropagation algorithm and the mean squared error performance function. This network achieved correlation of R=0.95. A reverse analysis was conducted using the optimised neural network. The analysis showed that the network is highly sensitive to changes in occupant height and weighted acceleration in Z axis direction - which coincides with previous work in ride comfort evaluation performed by other research teams.

Authors of this study recognize that the model derived based on the available dataset is not ideal. Presented study does not explore the field fully and future work is necessary to improve the robustness and accuracy of ride comfort estimation and prediction models based on neural networks. Limitations of the presented model mainly come from limited number of parameters. This study was designed as a proof of concept. In the future additional data collection is required to obtained much larger dataset which could be using to robustly train artificial neural networks for ride comfort evaluation and estimation. In the future, once the appropriate size dataset is gathered, it will be desirable to explore different, more advanced types of neural networks to optimize the performance of such comfort estimator. With increasing level of connectivity in vehicles, as well as raising number of parameters controlled, in the near future it will be possible to obtain live vehicle and passenger data. With high volumes of vehicles, algorithms for fast and robust data processing will be required. Therefore, it is vital to rethink the processes used for ride comfort evaluation. Overall it is concluded, that it is feasible to implement the neural

network methodology into the existing work flow based on ISO 2631:1997 standard. It is noted that this field is relatively unexplored. The further exploration is needed, with a richer set of sensors, and wider participation of human subjects.

Acknowledgements

This project is co-sponsored by HORIBA MIRA Ltd. and Coventry University and is a part of a PhD programme at Coventry University. Authors would like to thank HORIBA MIRA staff for participation in this research. We have no conflict of interest.

References

1. Warner JAC (1924) Riding Qualities Research
2. Hu Y, Chen MZQ, Sun Y (2017) Comfort-oriented vehicle suspension design with skyhook inerter configuration. J Sound Vib 405:34–47. https://doi.org/10.1016/j.jsv.2017.05.036
3. Kanarachos S, Dizqah AM, Chrysakis G, Fitzpatrick ME (2018) Optimal design of a quadratic parameter varying vehicle suspension system using contrast-based Fruit Fly Optimisation. Appl Soft Comput 62:463–477. https://doi.org/10.1016/J.ASOC.2017.11.005
4. Merker T, Girres G, Thriemer O (2002) Active Body Control (ABC) The DaimlerChrysler Active Suspension and Damping System. SAE International
5. Brown TL, Mear ST, Moore NE, et al (1992) An Experimental Procedure for Estimating Ride Quality for Passive and Semi-Active Suspension Automobiles. SAE International
6. Silveira M, Pontes BR, Balthazar JM (2014) Use of nonlinear asymmetrical shock absorber to improve comfort on passenger vehicles. J Sound Vib 333:2114–2129. https://doi.org/10.1016/j.jsv.2013.12.001
7. Eriksson J, Svensson L (2015) Tuning for ride quality in autonomous vehicle. 61
8. Fazlollahtabar H (2010) A subjective framework for seat comfort based on a heuristic multi criteria decision making technique and anthropometry. Appl Ergon 42:16–28. https://doi.org/10.1016/J.APERGO.2010.04.004
9. Kolich M (2008) A conceptual framework proposed to formalize the scientific investigation of automobile seat comfort. Appl Ergon 39:15–27. https://doi.org/10.1016/j.apergo.2007.01.003
10. Versace J (1959) Subjective Measurements in Engineering
11. Evans RD (1951) Riding Comfort
12. Pradko F, Orr TR, Lee RA (1965) Human Vibration Analysis. In: SAE Technical Paper 650426
13. Miwa T (1967) Evaluation methods for vibration effects part 2. Measurement of equal sensation level for whole body between vertical and horizontal sinusoidal vibrations. Ind Health 5:206–212. https://doi.org/10.2486/indhealth.5.206
14. Janeway RN (1975) Human Vibration Tolerance Criteria and Applications to Ride Evaluation. SAE International
15. Mehta NC (1981) Subjective and Objective Ride Evaluations of Commercial Vehicles. SAE International
16. Miller J (1981) A Subjective Assessment of Truck Ride Quality. In: SAE International Congress. SAE International

17. Schneider LW (1989) Survey of driver seating discomfort and related factors

18. Berger E, Gilmore BJ (1993) Seat Dynamic Parameters for Ride Quality. SAE International

19. Beard GF, Griffin MJ (2016) Discomfort of seated persons exposed to low frequency lateral and roll oscillation: Effect of backrest height. Appl Ergon 54:51–61. https://doi.org/10.1016/j.apergo.2015.11.010

20. Park J, Lee J, Ahn S, Jeong W (2017) Reduced ride comfort caused by beating idle vibrations in passenger vehicles. Int J Ind Ergon 57:74–79. https://doi.org/10.1016/j.ergon.2016.12.003

21. Meusch J, Rahmatalla S (2014) Whole-body vibration transmissibility in supine humans: Effects of board litter and neck collar. Appl Ergon 45:677–685. https://doi.org/10.1016/j.apergo.2013.09.007

22. Zhang X, Qiu Y, Griffin MJ (2015) Transmission of vertical vibration through a seat: Effect of thickness of foam cushions at the seat pan and the backrest. Int J Ind Ergon 48:36–45. https://doi.org/10.1016/j.ergon.2015.03.006

23. Bergman C, Castro PR, Högberg D, Hanson L (2015) Implementation of Suitable Comfort Model for Posture and Motion Prediction in DHM Supported Vehicle Design. Procedia Manuf 3:3753–3758. https://doi.org/10.1016/j.promfg.2015.07.816

24. Florin A, Manolache-Rusu I-C, Patuleanu L (2013) Pasive Suspension Modeling Using Matlab, Quarter Car Model, Input Signal Step Type. Teh - New Technol Prod Mach Manuf Technol

25. Geweda AE, El-Gohary MA, El-Nabawy AM, Awad T (2017) Improvement of vehicle ride comfort using genetic algorithm optimization and PI controller. Alexandria Eng J. https://doi.org/10.1016/j.aej.2017.05.014

26. Mustafa GIY, Wang HP, Tian Y (2018) Vibration control of an active vehicle suspension systems using optimized model-free fuzzy logic controller based on time delay estimation. Adv Eng Softw. https://doi.org/10.1016/J.ADVENGSOFT.2018.04.009

27. Goldman D (1948) A review of subjective responses to vibratory motion of the human body in the frequency range 1 to 70 cycles per second. Naval Medical Research Institute National Naval Medical Center, Bethesda Md.

28. Griffin MJ (1996) Handbook of Human Vibration. Elsevier

29. Mansfield NJ (2004) Human Response to Vibration. CRC Press

30. Lee RA, Pradko F (1968) Analytical Analysis of Human Vibration. SAE International

31. ISO 2631-1:1997 - Mechanical vibration and shock -- Evaluation of human exposure to whole-body vibration -- Part 1: General requirements. http://www.iso.org/iso/catalogue_detail.htm?csnumber=7612. Accessed 5 Nov 2015

32. Shurpali M V., Mullinix L (2011) An Approach for Validation of Suspension Seat for Ride Comfort using Multi-Body Dynamics. SAE International

33. Els PS (2005) The applicability of ride comfort standards to off-road vehicles. J Terramechanics 42:47–64. https://doi.org/10.1016/j.jterra.2004.08.001

34. Chaturvedi B, Rana D, Ravindran M (2010) Correlation of Vehicle Dynamics & amp; NVH Performance with Body Static & amp; Dynamic Stiffness through CAE and Experimental Analysis

35. Hiemstra-van Mastrigt S, Kamp I, van Veen SAT, et al (2015) The influence of active seating on car passengers' perceived comfort and activity levels. Appl Ergon 47:211–219. https://doi.org/10.1016/j.apergo.2014.10.004

36. Kudritzki DK (2001) Road Tests Adopted to Analyse Cars' Vibrational Behaviour. SAE International

37. Badiru I, Cwycyshyn WB (2013) Customer Focus in Ride Development. SAE International

38. Thite AN (2012) Development of a Refined Quarter Car Model for the Analysis of Discomfort due to Vibration. Adv Acoust Vib 2012:1–7. https://doi.org/10.1155/2012/863061

39. Mansfield N, Sammonds G, Nguyen L (2015) Driver discomfort in vehicle seats – Effect of changing road conditions and seat foam composition. Appl Ergon 50:153–159. https://doi.org/10.1016/j.apergo.2015.03.010

40. Nykänen A, Lennström D, Johnsson R (2015) Car Ride Before Entering the Lab Increases Precision in Listening Tests. SAE Int J Passeng Cars - Mech Syst 8:2015-01–2285. https://doi.org/10.4271/2015-01-2285

41. Schust M, Blüthner R, Seidel H (2006) Examination of perceptions (intensity, seat comfort, effort) and reaction times (brake and accelerator) during low-frequency vibration in x- or y-direction and biaxial (xy-) vibration of driver seats with activated and deactivated suspension. J Sound Vib 298:606–626. https://doi.org/10.1016/j.jsv.2006.06.029

42. Ebe K, Griffin MJ (2001) Factors affecting static seat cushion comfort. Ergonomics 44:901–21. https://doi.org/10.1080/00140130110064685

43. Gillespie TD (1992) Fundamentals of Vehicle Dynamics. SAE International

44. Versace J (1963) MEASUREMENT OF RIDE COMFORT

45. Kudritzki DK (2007) Ridemeter – Calculated Ride Comfort. SAE International

46. Kitazaki S, Griffin MJ (1997) Resonance behaviour of the seated human body and effects of posture. J Biomech 31:143–149. https://doi.org/10.1016/S0021-9290(97)00126-7

47. Kato K, Kitazaki S, Sonoda T (2009) Effects of Driver's Head Motion and Visual Information on Perception of Ride Comfort. SAE International

48. Kyung G, Nussbaum MA (2008) Driver sitting comfort and discomfort (part II): Relationships with and prediction from interface pressure. Int J Ind Ergon 38:526–538. https://doi.org/10.1016/j.ergon.2007.08.011

49. Elbanhawi M, Simic M, Jazar R (2015) In the Passenger Seat: Investigating Ride Comfort Measures in Autonomous Cars. IEEE Intell Transp Syst Mag 7:4–17. https://doi.org/10.1109/MITS.2015.2405571

50. Kolich M (2004) Predicting automobile seat comfort using a neural network. Int J Ind Ergon 33:285–293. https://doi.org/10.1016/j.ergon.2003.10.004

51. Blundell M, Harty D (2004) Multibody Systems Approach to Vehicle Dynamics. Elsevier

52. Zhao X, Schindler C (2014) Evaluation of whole-body vibration exposure experienced by operators of a compact wheel loader according to ISO 2631-1:1997 and ISO 2631-5:2004. Int J Ind Ergon 44:840–850. https://doi.org/10.1016/j.ergon.2014.09.006

53. Little E, Handrickx P, Grote P, et al (1999) Ride Comfort Analysis: Practice and Procedures. SAE International

54. (2014) J1060 - Subjective Rating Scale for Evaluation of Noise and Ride Comfort Characteristics Related to Motor Vehicle Tires

55. Kim H-J, Martin BJ (2007) Estimation of Body Links Transfer Functions in Vehicle Vibration Environment. SAE International

56. Kyung G, Nussbaum MA, Babski-Reeves K (2008) Driver sitting comfort and discomfort (part I): Use of subjective ratings in discriminating car seats and correspondence among ratings. Int J Ind Ergon 38:516–525. https://doi.org/10.1016/j.ergon.2007.08.010

57. Gurram R, Vértiz AM (1997) The Role of Automotive Seat Cushion Deflection in Improving Ride Comfort. SAE International

58. Tuluie R, Stewart G (1999) Motorcycle Suspension Development Using Ride Comfort Analysis with a Laboratory Test System

59. Dewangan K, Rakheja S, Marcotte P (2018) Gender and anthropometric effects on whole-body vibration power absorption of the seated body. J Low Freq Noise, Vib Act Control 37:167–190. https://doi.org/10.1177/1461348418780017

60. Lundström R, Holmlund P, Lindberg L (1998) Absorption of energy during vertical whole-body vibration exposure. J Biomech 31:317–326. https://doi.org/10.1016/S0021-9290(98)00011-6

61. Adam SA, Jalil NAA (2017) Vertical Suspension Seat Transmissibility and SEAT Values for Seated Person Exposed to Whole-body Vibration in Agricultural Tractor Preliminary Study. In: Procedia Engineering

62. Kolich M, Seal N, Taboun S (2004) Automobile seat comfort prediction: statistical model vs. artificial neural network. Appl Ergon 35:275–284. https://doi.org/10.1016/j.apergo.2004.01.007

63. Nima E (2008) Development of a Semi-active Intelligent Suspension System for Heavy Vehicles

64. Lerspalungsanti S, Albers A, Ott S, Düser T (2015) HUMAN RIDE COMFORT PREDICTION OF DRIVE TRAIN USING MODELING METHOD BASED ON ARTIFICIAL NEURAL NETWORKS. Int J Automot Technol 16:153–166. https://doi.org/10.1007/s12239−015−0017−2

65. Sarawut L, Albert A, Sascha O (2013) Subjective Evaluation and Modeling of Human Ride Comfort of Electric Vehicle Using Tools Based on Artificial Neural Networks. Springer, Berlin, Heidelberg, pp 1777–1785

66. Gao Y, Tang R, Liang J, et al (2010) Evaluation of vehicle ride comfort based on neural network. International Society for Optics and Photonics, p 754407

67. Taghavifar H, Rakheja S (2018) Supervised ANN-assisted modeling of seated body apparent mass under vertical whole body vibration. Measurement 127:78–88. https://doi.org/10.1016/J.MEASUREMENT.2018.05.092

68. Nybacka M, He X, Su Z, et al (2014) Links between subjective assessments and objective metrics for steering, and evaluation of driver ratings. Veh Syst Dyn 52:31–50. https://doi.org/10.1080/00423114.2013.876503

69. McCulloch WS, Pitts W (1943) A logical calculus of the ideas immanent in nervous activity. Bull Math Biophys 5:115–133. https://doi.org/10.1007/BF02478259

70. Sydenham PH, Thorn R (2005) Handbook of measuring system design. Wiley

71. Gill PE, Murray W, Wright MH (1981) Practical optimization. Academic Press

72. Møller MF, Møller MF (1993) A scaled conjugate gradient algorithm for fast supervised learning. NEURAL NETWORKS 6:525--533

73. Ajith Abraham, Sydenham PH, Thorn R (2005) Artificial Neural Networks. In: Handbook of measuring system design. pp 900–909